$M_{4,5}N_{4,5}X$ Auger electron spectra of iodine and xenon. Many-body effects

S. Aksela and H. Aksela
Department of Physics, University of Oulu, SF-90100 Oulu 10, Finland

T. D. Thomas
Department of Chemistry and Radiation Center, Oregon State University, Corvallis, Oregon 97331

(Received 27 June 1978)

High-resolution $M_{4,5}N_{2,3}N_{4,5}$, $M_{4,5}N_{4,5}N_{4,5}$, and $M_{4,5}N_{4,5}O$ Auger spectra from I_2 vapor and from Xe gas have been measured using electron-beam excitation. In order to reduce satellite backgrounds, the $M_{4,5}N_{4,5}N_{4,5}$ spectra were also taken using primary-beam energies just below the core-ionization energy of the M_3 levels of iodine and xenon. The relative line energies and intensities for all of the xenon spectra and for iodine $M_{4,5}N_{4,5}N_{4,5}$ spectra have been calculated in the mixed-coupling scheme. The agreement between theory and experiment is excellent for the $M_{4,5}N_{4,5}N_{4,5}$ spectra of both xenon and iodine. The agreement for the xenon $M_{4,5}N_{2,3}N_{4,5}$ spectrum is less good, but is close enough to indicate the approximate validity of the independent-electron model. This result is in contrast to that for one-hole states involving the $N_{2,3}$ shell; such a model fails completely to account for the xenon $4p$ photoemission spectrum. The independent-electron model will not account for the $M_{4,5}N_{2,3}N_{4,5}$ spectrum of iodine. Reasons for the success of this model for xenon and its failure for iodine are presented. The observed inherent linewidths of the Auger lines are considerably broader in molecular iodine than in xenon. The photoelectron spectra and core-ionization energies of the $3d$, $4s$, $4p$, $4d$, $5s$, and $5p$ levels of I_2 have been measured. The role of extra-atomic relaxation in the observed Auger energies is discussed.

I. INTRODUCTION

Auger-electron spectra provide tests of theories of electronic structure. The Auger kinetic energies depend on the energies of the one- and two-hole states in the atom or molecule of interest, and hence provide information on the coupling of pairs of electrons or pairs of holes. The relative intensities of the various Auger electrons depend on matrix elements between initial and final states, and therefore provide information on the quality of the wave functions.

The most accurate Auger spectra are those measured in the gas phase. For measurements in solids, the lines are usually significantly broadened because of the vibrational excitation of the solid during core ionization and during the Auger process. This broadening is nonexistent for gas phase atoms and usually smaller for gas phase molecules than for the same species in the solid phase. In addition, measurements of absolute energies in solids are usually hampered by lack of knowledge about reference levels and charging effects.

The number of atomic species that can be conveniently obtained in the gas phase at room temperature is small; the noble gases and mercury. At somewhat higher temperatures it has been possible to make gas phase measurements on the alkali metals, on the alkaline earth metals, and on zinc and cadmium. For molecules a number of gas phase species are available, making it possible to study elements other than those mentioned above. If the final two-hole states are in the atomic core, presumably the Auger spectra for free molecules are about the same as those for the free atoms, except for effects due to extra-atomic relaxation and vibrational broadening.

The $M_{4,5}N_{4,5}N_{4,5}$ Auger spectra of Xe and I_2 provide further tests of the theory that has been used to calculate Auger intensities and energies. The I_2 measurements test the validity of free-atom calculations for a molecule in the case that the valence electrons are not directly involved in the Auger process. A comparison between the results for Xe and those for I_2 shows the effects on an inner-shell Auger spectrum of an adjacent spectator atom—line broadening due to vibrational excitation and a shift due to extra-atomic relaxation.

The $M_{4,5}N_{2,3}N_{4,5}$ and $M_{4,5}N_{4,5}O$ spectra are presented and discussed for both of these elements. The $M_{4,5}N_{2,3}N_{4,5}$ spectra are of particular interest since they involve a hole in the $4p$ shell. For singly ionized xenon and iodine, these states cannot be accurately described by an independent-particle picture. There is considerable broadening of the levels because of the possibility of super Coster-Kronig transitions; because of extensive configuration mixing with $4d^8 4f$ configurations the single-particle strength is spread over many levels. By contrast, the xenon $M_{4,5}N_{2,3}N_{4,5}$ Auger spectrum is described more or less adequately by an independent-particle model. On the other hand, it is clear from a comparison of the iodine and

xenon experimental spectra and from a comparison of experimental and theoretical results for iodine that such a model will not adequately describe the iodine Auger spectrum.

The $M_{4,5}N_{4,5}N_{4,5}$ Auger-electron spectrum of xenon has been studied recently by Hagmann *et al.*[1] and Werme *et al.*,[2] who used 4–5-keV electrons to ionize the xenon atoms. With such a high primary-beam energy ionization of the 3*s* and 3*p* core electrons is also possible; because of the high Coster-Kronig transition probabilities these ionizations lead to double-hole states $M_{4,5}X$ (with $X=N$ or O), which produce $M_{4,5}X$-$N_{4,5}N_{4,5}X$ satellite Auger spectra. The energies of these satellite Auger lines are only a few eV lower than those of the diagram Auger lines and they are thus overlapping with the diagram spectrum. This effect complicates the reliable background subtraction, especially under the $M_5N_{4,5}N_{4,5}$ line group. Therefore, we have tried to reduce this complicated satellite background by exciting the $M_{4,5}N_{4,5}N_{4,5}$ Auger spectra of Xe and I_2 with such low primary-beam energies that the deeper lying $M_{2,3}$ levels cannot be ionized. In this case, a strong reduction in the intensity of satellite lines is expected. The only remaining mechanisms by which the satellite lines can be created are shake-off and shake-up processes. Because the cross section for electron-impact ionization[3] of inner-shell electrons decreases rapidly with decreasing kinetic energy of the primary beam near the ionization threshold and because the intensity of inelastically scattered primary electrons increases with decreasing energy of the primary beam, a high-transmission electron spectrometer is needed for this kind of experiment.

The $M_{4,5}N_{2,3}N_{4,5}$ and $M_{4,5}N_{4,5}O_{1,2,3}$ Auger-electron spectra of xenon have been measured by Werme *et al.*, but no detailed interpretations of the line components of these very complicated groups have been done until now. In connection with these investigations we have measured the 3*d*, 4*s*, 4*p*, 4*d*, 5*s*, and 5*p* ionization potentials of I_2. The comparison between the core-ionization potentials and the kinetic energies of the Auger electrons from Xe and I_2 makes it possible to estimate the contribution of the extra-atomic relaxation to the measured kinetic energies of the iodine Auger electrons.

II. EXPERIMENTAL PROCEDURES AND RESULTS

The measurements of the Auger spectra of I_2 and Xe and the photoelectron spectra of I_2 were made in a cylindrical mirror electrostatic analyzer.[4] The $M_{4,5}N_{4,5}N_{4,5}$ Auger electrons were excited by incident electrons with energies of both 3 keV and about 900 eV (880 for iodine and 900 for xenon). The photoelectron spectra were taken using Al $K\alpha$ x rays. The mean emission angle of the measured Auger electrons with respect to the direction of the primary beam, parallel to the symmetry axis of the cylinders, is 60° in this spectrometer. The iodine vapor was obtained by letting solid iodine evaporate at room temperature and flow into the sample cell of the spectrometer. The gas pressure in the sample cell of the spectrometer was about 10^{-3} Torr. The standard pulse counting method has been used.

The energy resolution of the spectrometer was 0.09% or 0.47-eV full width at half-maximum (FWHM) for the measured $M_{4,5}N_{4,5}N_{4,5}$ Auger spectra. This quantity was determined by least-squares fits of Voigt functions to the Ne KLL (^1D) and Ar $L_3M_{2,3}M_{2,3}$ ($^1S_0$) Auger spectra, whose energies bracket the energies of interest here, and from the experimental values of the intrinsic linewidths for these transitions. These measurements also show that the spectrometer resolution function is with good accuracy a Gaussian function when the full 2π circular aperture is used.

A. $M_{4,5}N_{4,5}N_{4,5}$ spectra

The experimental $M_{4,5}N_{4,5}N_{4,5}$ Auger spectra of iodine and xenon are shown in Figs. 1 and 2. In each case, curve (a) shows the result using 3-keV excitation and curve (b) shows that using 0.9-keV excitation. The peak-to-background ratio was found to be much lower for lower primary-beam energies and the overall backgrounds have differ-

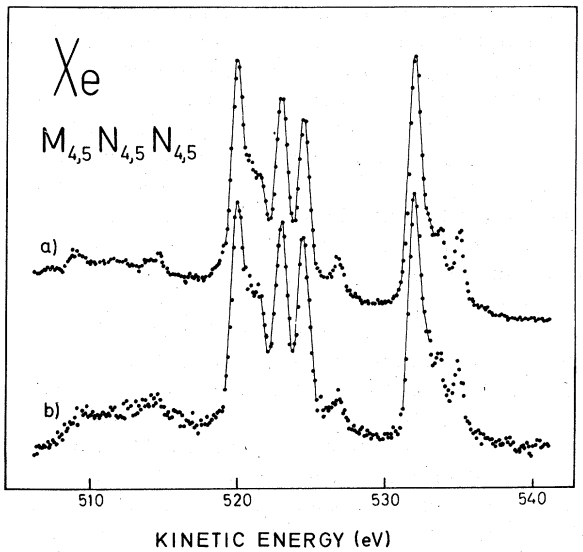

FIG. 1. $M_{4,5}N_{4,5}N_{4,5}$ Auger-electron spectrum of xenon excited (a) with 3-keV electrons and (b) with 900-eV electrons.

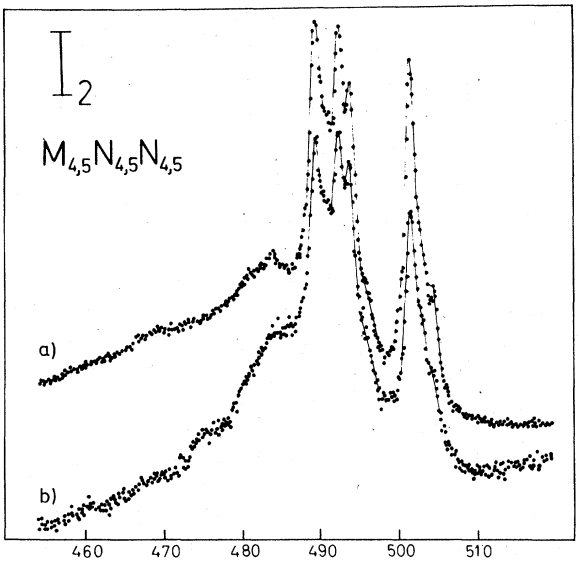

FIG. 2. $M_{4,5}N_{4,5}N_{4,5}$ Auger-electron spectrum of iodine excited (a) with 3-keV electrons and (b) with 880-eV electrons.

ent slopes; the main features of the spectra are, however, the same. The line groups are accompanied on the low-energy side by rather high background, which is especially strong in the case of molecular iodine. This background originates mainly from satellite Auger transitions and from inelastically scattered Auger and primary-beam electrons. The method of subtracting this background before decomposing the line groups into their components is of crucial importance and may cause the largest uncertainty in the intensities of the line components. In this study we have used a linear background with different slopes under the M_4 and M_5 groups, adjusting the heights of background on the high- and low-energy sides of the groups and at the minimum between the groups. Spectra corrected for background are shown in Figs. 3 and 4. That the Auger lines for I_2 are broader than the corresponding lines for Xe is quite noticeable.

The line groups have been fit by least squares using six components in each group and keeping the relative separations of the components the same in the two groups. As noted above, Ne and Ar Auger spectra were measured to determine the spectrometer resolution function. This was convoluted with a Lorentzian line shape, describing the inherent line shape of Auger lines, to get the line that gives the best fit to the experimental spectrum. The fits are shown as the solid curves in Figs. 3 and 4. The positions and intensities are represented by the vertical lines.

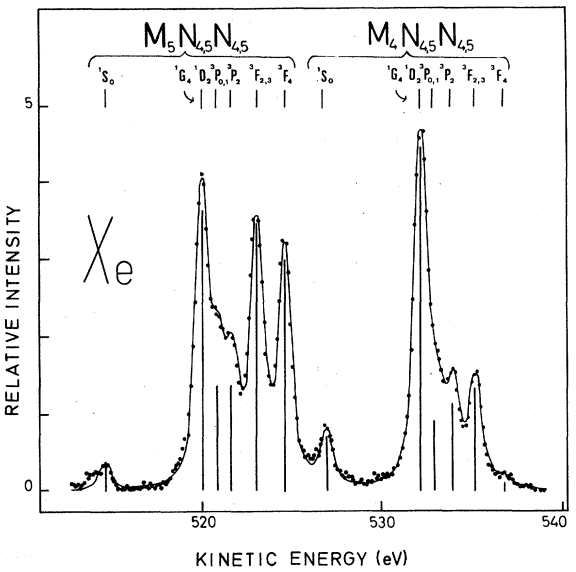

FIG. 3. $M_{4,5}N_{4,5}N_{4,5}$ Auger spectrum of xenon excited with 3-keV electrons after background subtraction and dispersion correction. The solid curve and vertical lines represent a least-squares fit of standard functions (convolution of spectrometer function with Lorentz profile) to the data. The configuration assignments refer to calculations carried out in LS coupling.

The results of the fits are given in Tables I–IV. The energies are given relative to the strong $^1G_4$ component. The intensities are given in percent of the total intensity of the corresponding group.

The energy calibration of the iodine $M_{4,5}N_{4,5}N_{4,5}$ Auger spectrum was done using Ne KLL ($^1S_0$) (804.557 ± 0.017 eV)[5] and Ar $L_3M_{2,3}M_{2,3}$ ($^1D_2$) (201.10 ± 0.05 eV)[5-7] lines and also with the aid

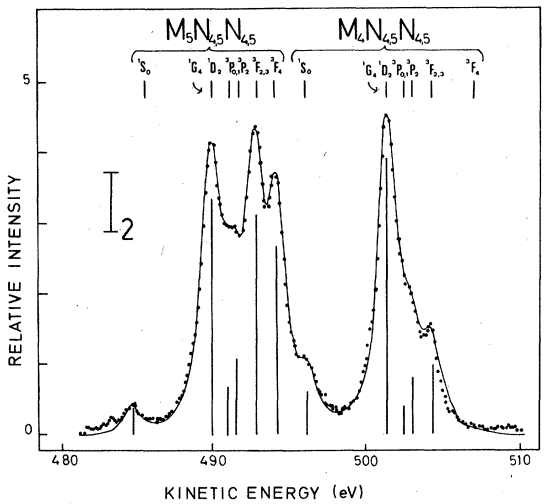

FIG. 4. Separation of the $M_{4,5}N_{4,5}N_{4,5}$ spectrum of iodine into its components. See caption to Fig. 3.

TABLE I. Theoretical and experimental energies (in eV) of the $M_{4,5}N_{4,5}N_{4,5}$ Auger lines of Xe relative to the state $^1G_4$. Column a, *LS* coupling plus diagonal contributions from the spin-orbit interaction. Column b, intermediate coupling.

Assignment of final state	Theory a	Theory b	Experiment
$^1S_0$	−5.67	−6.13	−5.71
$^1D_2$	1.30	−0.06	0.00
$^1G_4$	0.00	0.00	
$^3P_1$	0.57	0.70	0.92
$^3P_0$	0.18	0.89	
$^3P_2$	2.17	1.84	1.72
$^3F_2$	1.36	3.42	3.15
$^3F_3$	3.35	3.48	
$^3F_4$	4.93	5.18	4.76

TABLE II. Theoretical and experimental energies (in eV) of the $M_{4,5}N_{4,5}N_{4,5}$ Auger lines of I_2 relative to the state $^1G_4$. Column a, *LS* coupling plus diagonal contributions from the spin-orbit interaction. Column b, intermediate coupling.

Assignment of final state	Theory a	Theory b	Experiment
$^1S_0$	−5.39	−5.76	−5.18
$^1G_4$	0.00	0.00	
$^1D_2$	1.24	0.06	0.00
$^3P_1$	0.57	0.68	1.02
$^3P_0$	0.23	0.80	
$^3P_2$	2.19	1.76	1.64
$^3F_2$	1.26	3.18	2.90
$^3F_3$	3.23	3.33	
$^3F_4$	4.61	4.81	4.34

of reported energies for the xenon $M_{4,5}N_{4,5}N_{4,5}$ spectrum.[2] Both energy calibrations agree rather well and give 506.70 ± 0.15 eV for the $M_4N_{4,5}N_{4,5}$ ($^1G_4$) line of I_2. The M_4-M_5 spin-orbit splitting obtained from the Auger spectrum is 11.45 ± 0.05 eV. For the inherent widths (FWHM) of the Auger lines, we have determined 0.92 ± 0.05 eV for I_2 and 0.64 ± 0.05 eV for Xe, assuming, as noted above, that the line shape is Lorentzian.[8]

B. Other $M_{4,5}$ Auger spectra and photoelectron spectra

The $M_{4,5}N_{2,3}N_{4,5}$ Auger spectra of xenon and iodine are shown in Fig. 5. The spectrum of xenon after background subtraction is shown in Fig. 6; the solid line represents the fit to the data. The results for xenon from the decomposition are given in Tables V and VI. The results for $M_{4,5}N_{4,5}O$ spectra are given in Figs. 7 and 8 and for xenon in Tables VII and VIII.

The $3d_{3/2,5/2}$, $4s$, $4p$, $4d_{3/2,5/2}$, $5s$ and $5p$ photoelectron lines of I_2 were measured using Al $K\alpha$ radiation. The spectra after smoothing over 5 points are shown in Fig. 9. The values obtained for the ionization potentials are given in Table IX. The energy calibration was done against the Ne 1*s* and 2*s* and Ar 3*p* photolines. The 3*d* and 4*d* spin-orbit splittings from these photoelectron measure-

TABLE III. Theoretical and experimental relative intensities (in percent) of the $M_{4,5}N_{4,5}N_{4,5}$ Auger lines of Xe. Column a, *LS* coupling for final state. Column b, intermediate coupling for final state. Column c, experimental spectrum excited by 3-keV electrons. Column d, spectrum excited by 900-eV electrons.

Transition		Theory a		Theory b		Experiment c	Experiment d
$M_5N_{4,5}N_{4,5}$	$^1S_0$	3.5		2.1		2.6	3.6
	$^1D_2$	12.4	37.7	4.0	27.1	28.2	25.7
	$^1G_4$	25.3		23.1			
	$^3P_1$	5.9	7.5	5.9	8.9	10.4	11.0
	$^3P_0$	1.6		3.0			
	$^3P_2$	3.3		9.9		10.4	11.9
	$^3F_2$	13.7	24.2	15.5	26.0	25.3	24.5
	$^3F_3$	10.5		10.5			
	$^3F_4$	23.8		26.0		23.1	23.2
$M_4N_{4,5}N_{4,5}$	$^1S_0$	3.5		5.5		8.2	8.0
	$^1D_2$	12.4	37.7	23.3	51.2	51.7	49.7
	$^1G_4$	25.3		27.9			
	$^3P_1$	8.8	12.3	8.8	10.4	10.4	13.4
	$^3P_0$	3.5		1.6			
	$^3P_2$	17.5		11.9		13.1	13.2
	$^3F_2$	8.8	24.3	3.5	19.0	15.3	14.2
	$^3F_3$	15.5		15.5			
	$^3F_4$	4.6		1.9		1.4	1.6

TABLE IV. Theoretical and experimental relative intensities (in percent) of the $M_{4,5}N_{4,5}N_{4,5}$ Auger lines of I_2. Column a, LS coupling for final state. Column b, intermediate coupling for final state. Column c, experimental spectrum excited by 3-keV electrons. Column d, spectrum excited by 880-eV electrons.

Transition		Theory a		Theory b		Experiment c	Experiment d
$M_5N_{4,5}N_{4,5}$	$^1S_0$	3.8		2.4		4.7	3.0
	$^1G_4$	25.5	38.0	23.5	27.8	30.4	28.1
	$^1D_2$	12.5		4.3			
	$^3P_1$	5.9	7.5	5.9	8.9	6.5	8.6
	$^3P_0$	1.6		3.0			
	$^3P_2$	3.2		10.6		8.9	7.6
	$^3F_2$	13.8	24.2	14.6	25.0	26.8	27.9
	$^3F_3$	10.4		10.4			
	$^3F_4$	23.5		25.5		22.8	24.8
$M_4N_{4,5}N_{4,5}$	$^1S_0$	3.8		5.7		8.6	11.5
	$^1G_4$	25.5	38.0	28.0	51.1	58.7	52.6
	$^1D_2$	12.5		23.1			
	$^3P_1$	8.9	12.5	8.9	10.6	6.9	10.5
	$^3P_0$	3.6		1.7			
	$^3P_2$	17.3		11.3		11.6	10.7
	$^3F_2$	8.9	24.2	4.3	19.6	13.8	13.4
	$^3F_3$	15.3		15.3			
	$^3F_4$	4.4		1.9		0.4	1.1

ments are 11.50 ± 0.05 eV (in agreement with that obtained from the Auger spectrum) and 1.7 ± 0.1 eV, respectively.

III. THEORETICAL CALCULATIONS

For the theoretical calculations of energies and intensities we follow the same procedure that has been used by Aksela *et al.* for the $N_{6,7}O_{4,5}O_{4,5}$ spectrum of mercury,[9] the $M_{4,5}N_{4,5}N_{4,5}$ spectrum of cadmium[10] and the $L_{2,3}M_{4,5}M_{4,5}$ spectrum of zinc.[11] A detailed description of the procedure will be given elsewhere.[12] In the light of studies about xenon[1] and cadmium[10] it is clear that the mixed coupling scheme applying jj coupling for the initial state and intermediate coupling for the final state is the proper one to calculate the relative energies and intensities of the line components.

In the calculations of the energies of the final-

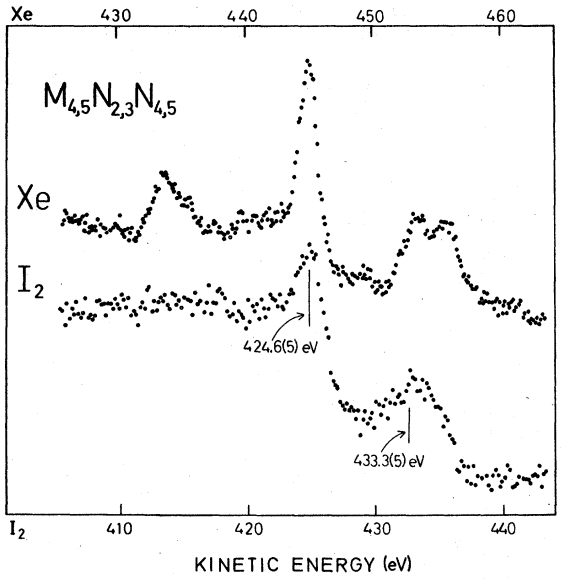

FIG. 5. $M_{4,5}N_{2,3}N_{4,5}$ Auger-electron spectra of Xe and I_2 excited with 3-keV electrons.

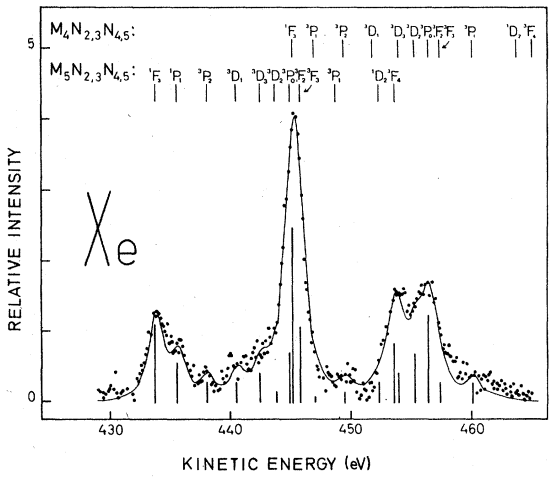

FIG. 6. Separation of the $M_{4,5}N_{2,3}N_{4,5}$ spectrum of xenon into its components. See caption to Fig. 3.

TABLE V. Theoretical and experimental energies (in eV) of Xe relative to the state $^1F_3$ of the $M_{4,5}N_{2,3}N_{4,5}$ transitions. Column a, *LS* coupling plus diagonal contributions from the spin-orbit interaction. Column b, intermediate coupling.

Transition		Theory a	Theory b	Experiment
$M_{4,5}N_{2,3}N_{4,5}$	$^1F_3$	0.00	0.00	0.00
	$^1P_1$	1.36	0.14	1.95
	$^3P_2$	10.21	5.67	4.55
	$^3D_1$	5.99	6.39	7.15
	$^3D_3$	11.07	13.63	9.36
	$^3D_2$	12.71	15.18	10.66
	$^3P_0$	13.16	15.63	11.83
	$^3F_2$	9.36	16.34	
	$^3F_3$	14.30	19.15	13.00
	$^3P_1$	11.69	19.92	16.02
	$^1D_2$	14.78	21.49	19.89
	$^3F_4$	20.85	23.33	20.93

state levels in intermediate coupling we have used *LS* wave functions for a basis set; the true wave functions are linear combinations of the members of this basis set. Coulomb matrix elements for the construction of the energy matrices are taken from Slater[13] and spin-orbit elements from Condon and Shortley.[14] For the numerical values of Slater integrals we have used the values tabulated by Mann[15] from Hartree-Fock calculations. The numerical values for the spin-orbit parameter are obtained from theoretical calculations of Huang *et al.*[16] The calculated energies relative to the most intense line component of the group are given in Tables I, II, V, and VII.

The intensities of the lines are calculated applying *jj* coupling to the initial state and intermediate coupling to the final states. The transition amplitudes in *LS* coupling are calculated using expressions of Shore and Menzel[17] as functions of the radial integrals $D(\lambda, l')$ and $E(\lambda, l')$. With the aid of transformation coefficients from *LS* coupling in final and initial states to *LS* coupling in the final state and *jj* coupling in the initial state, the transition amplitudes in mixed coupling are then calculated, and using the mixing coefficients obtained from the eigenvectors of the energy matrices the transition rates of different Auger components are finally calculated. The numerical values of radial integrals are obtained from the values calculated by McGuire[18] with HFS wave functions. The relative intensities are given in Tables III, IV, VI, and VIII.

In the calculations the passive shells have been neglected and only the shells participating in the Auger process have been taken into consideration.

TABLE VI. Theoretical and experimental relative intensities (in percent) of the $M_{4,5}N_{2,3}N_{4,5}$ transitions of Xe. Column a, *LS* coupling for final state. Column b, intermediate coupling for final state.

Transition		Theory a		Theory b		Experiment
$M_5N_{2,3}N_{4,5}$	$^1F_3$	27.0	36.5	16.5	20.8	30.6
	$^1P_1$	9.5		4.3		
	$^3P_2$	11.9		2.5		5.4
	$^3D_1$	0.8		8.2		5.9
	$^3D_3$	18.2		22.0		6.3
	$^3D_2$	6.0		11.9		
	$^3P_0$	0.0	6.7	0.0	13.5	16.5
	$^3F_2$	0.7		1.6		
	$^3F_3$	5.1	7.5	11.8	12.0	14.3
	$^3P_1$	2.4		0.2		
	$^1D_2$	4.9		7.5		6.4
	$^3F_4$	13.5		13.5		14.6
$M_4N_{2,3}N_{4,5}$	$^3F_3$	27.0	36.5	34.2	48.1	46.2
	$^1P_1$	9.5		13.9		
	$^3P_2$	2.0		14.8		2.6
	$^3D_1$	11.3		1.9		0.0
	$^3D_3$	1.9		1.0		8.2
	$^3D_2$	11.9		0.7		
	$^3P_0$	4.0	26.3	4.0	15.8	32.8
	$^3F_2$	10.4		11.1		
	$^3F_3$	8.4	16.7	2.2	15.5	10.2
	$^3P_1$	8.3		13.3		
	$^1D_2$	4.9		2.5		0.0
	$^3F_4$	0.4		0.4		0.0

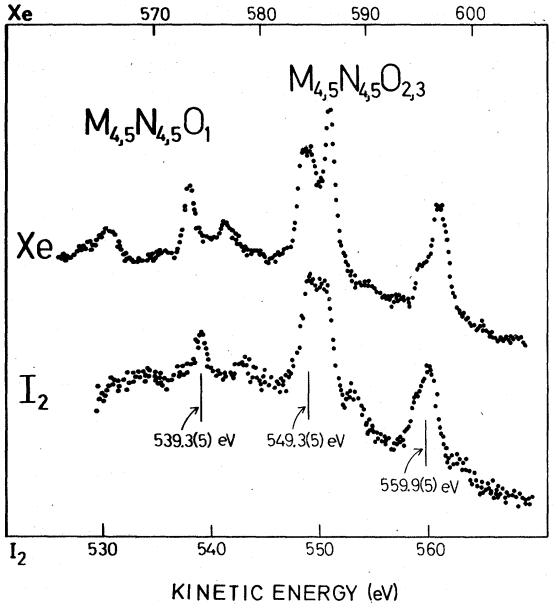

FIG. 7. $M_{4,5}N_{4,5}O_{1,2,3}$ Auger electron spectra of Xe and I_2 excited with 3-keV electrons.

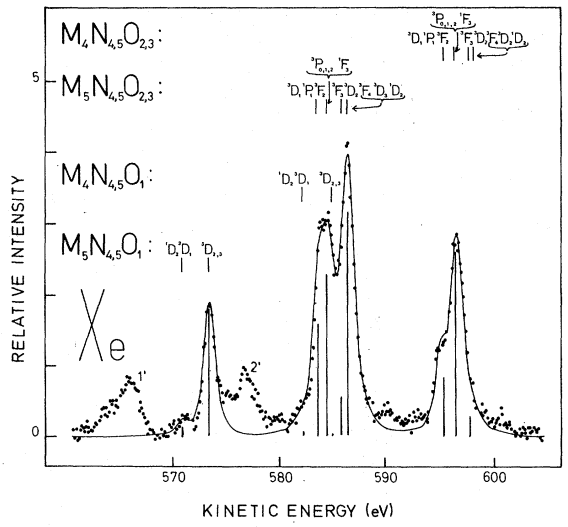

FIG. 8. Decomposition of the $M_{4,5}N_{4,5}O_{1,2,3}$ spectrum of xenon. Peaks 1′ and 2′ are thought to be satellites. See also the caption to Fig. 3.

IV. DISCUSSION

A. $M_{4,5}N_{4,5}N_{4,5}$ spectra

Our experimental results for the relative intensities of line components in the $M_4N_{4,5}N_{4,5}$ and $M_5N_{4,5}N_{4,5}$ groups of xenon and iodine spectra show that the differences between 0.9 and 3-keV excitation are generally small. In the M_5 group the total intensity of overlapping $^1G_4$ and $^1D_2$ components is slightly higher for 3-keV than for 0.9-keV excitation both in xenon and iodine. Other differences in the M_5 group are not significant within the accuracy of the deconvolution procedure used for this group of many overlapping lines. Also in the M_4 group the intensities of the $^1G_4$ and $^1D_2$ components are higher and of the $^3P_{0,1}$ components lower for high-energy than for low-energy excitation. This may be an indication of some structure with rather low intensity below the $^1G_4$ and $^1D_2$ components in the case of high-energy excitation.

Comparison of our experimental results with those of Hagmann *et al.*[1] and Werme *et al.*[2] shows that our relative intensities agree well with the values of Hagmann *et al.*, but deviate from those of Werme *et al.* especially for the stronger components of the groups. Hagmann *et al.* have calculated the satellite background theoretically using a trapezoidally shaped continuous distribution for each satellite group, $M_{4,5}O_i$-$N_{4,5}N_{4,5}O_i$ and $M_{4,5}N_i$-$N_{4,5}N_{4,5}N_i$. Their sum satellite distribution reaches the plateau under the ^3F components of the M_5 group thus somewhat earlier than does our simple linear approximation.

For the group intensity ratio $(M_4N_{4,5}N_{4,5})/(M_5N_{4,5}N_{4,5})$ in Xe spectra we obtain 0.67 and 0.60 for 3-keV and 900-eV excitation, respectively. The high-energy value is thus equal to the statistical ratio $\frac{4}{6}$. The observed inherent width of 0.64 eV in the $M_{4,5}N_{4,5}N_{4,5}$ spectrum of xenon agrees well with the value of 0.65 eV of Hagmann *et al.*[1] and with the $M_{4,5}$ and $N_{4,5}$ level widths of

TABLE VII. Theoretical and experimental energies (in eV) of Xe relative to the state $^1D_2$ of the $M_{4,5}N_{4,5}O_1$ transitions and to the state F_3 of the $M_{4,5}N_{4,5}O_{2,3}$ transitions. Column a, *LS* coupling plus diagonal contributions from the spin-orbit interaction. Column b, intermediate coupling.

Transition		Theory a	Theory b	Experiment
$M_{4,5}N_{4,5}O_1$	$^1D_2$	0.00	0.00	0.00
	$^3D_1$	−0.60	0.28	
	$^3D_2$	0.19	1.94	2.80
	$^3D_3$	1.38	2.25	
$M_{4,5}N_{4,5}O_{2,3}$	$^3D_1$	−0.07	−1.07	−1.56
	$^1P_1$	−0.39	−1.05	
	$^3F_2$	−0.88	−0.81	−0.91
	$^3P_1$	−0.19	−0.18	0.00
	$^3P_0$	−0.55	−0.15	
	$^1F_3$	0.00	0.00	
	$^3P_2$	0.18	0.28	
	$^3F_3$	0.35	0.91	1.43
	$^3D_2$	0.74	0.96	
	$^3F_4$	1.99	2.39	2.08
	$^3D_3$	1.94	2.57	
	$^1D_2$	1.36	2.57	

TABLE VIII. Theoretical and experimental relative intensities (in percent) of the $M_{4,5}N_{4,5}O_1$ and $M_{4,5}N_{4,5}O_{2,3}$ transitions of Xe. Column a, *LS* coupling for final state. Column b, intermediate coupling for final state.

Transition		Theory a		Theory b		Experiment
$M_5N_{4,5}O_1$	$^1D_2$	40.3	40.9	7.7	8.3	8.0
	$^3D_1$	0.6		0.6		
	$^3D_2$	13.6	59.1	46.2	91.7	92.0
	$^3D_3$	45.5		45.5		
$M_4N_{4,5}O_1$	$^1D_2$	40.3	69.3	66.2	95.2	68.4
	$^3D_1$	29.0		29.0		
	$^3D_2$	29.4	30.7	3.5	4.8	31.6
	$^3D_3$	1.3		1.3		
$M_5N_{4,5}O_{2,3}$	$^3D_1$	0.8	10.4	0.6	11.3	18.5
	$^1P_1$	8.8		9.9		
	$^3F_2$	0.8		0.8		
	$^3P_1$	2.4	38.3	1.6	38.6	25.9
	$^3P_0$	0.0		0.0		
	$^1F_3$	23.8		26.3		
	$^3P_2$	12.1		10.7		
	$^3F_3$	5.8	11.9	0.4	7.9	9.8
	$^3D_2$	6.1		7.5		
	$^3F_4$	15.4	39.3	15.4	42.3	45.9
	$^3D_3$	18.4		21.3		
	$^1D_2$	5.5		5.6		
$M_4N_{4,5}O_{2,3}$	$^3D_1$	11.4	32.0	12.4	28.2	26.3
	$^1P_1$	8.8		3.4		
	$^3F_2$	11.8		12.4		
	$^3P_1$	8.5	38.3	12.9	30.6	64.8
	$^3P_0$	4.0		4.0		
	$^1F_3$	23.8		11.2		
	$^3P_2$	2.0		2.5		
	$^3F_3$	9.6	21.6	23.9	33.2	8.9
	$^3D_2$	12.0		9.3		
	$^3F_4$	0.5	8.0	0.5	8.0	0.0
	$^3D_3$	2.0		0.4		
	$^1D_2$	5.5		7.1		

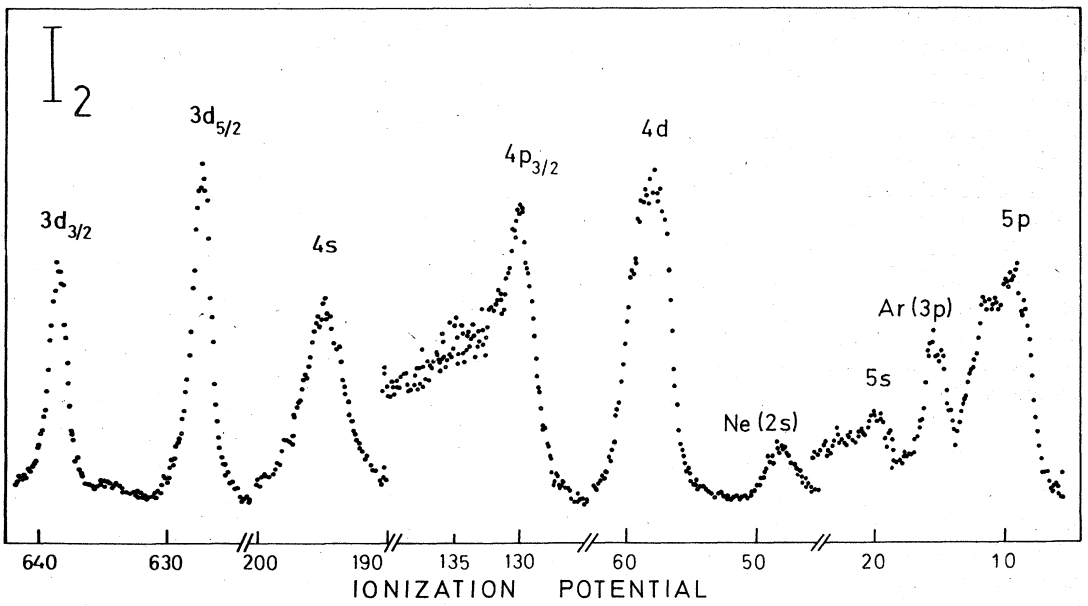

FIG. 9. Photoelectron spectra of I_2 excited by Al $K\alpha$ radiation.

TABLE IX. Experimental ionization potentials (in eV) for I_2.

Level	Ionization potential
$3d_{3/2}$	638.7(2)
$3d_{5/2}$	627.2(2)
$4s$	194.8(2)
$4p_{3/2}$	129.9(5)
$4d_{3/2}$	59.2(2)
$4d_{5/2}$	57.5(2)
$5s$	20.0(5)
$5p$	11.0(5)

0.5 and 0.1 eV obtained from the photoelectron spectra of xenon.[22] A theoretical value of 0.63 eV for the total width of the M_4 and M_5 levels has been calculated by McGuire.[23] Combining this with an estimate by Hagmann *et al.*[1] of 0.18 eV for the width of the $N_{4,5}N_{4,5}$ final states gives 0.8 eV for the inherent width of the $M_{4,5}N_{4,5}N_{4,5}$ Auger transitions. This is clearly more than the observed values.

Comparison between the experimental and calculated relative energies and intensities for iodine shows that the use of intermediate coupling improves the agreement considerably. The general agreement is quite good and is of the same quality that has been found earlier for Xe and Cd.[1,10] A graphical comparison between experiment and theory for xenon and iodine is shown in Figs. 10 and 11. In the first of these we show a direct comparison between calculated and measured energies and intensities. In the second we have plotted theoretical versus experimental intensity. The agreement between experiment and theory is excellent, indicating that configuration interaction does not play a strong role in these spectra. The agreement is as good for iodine as for xenon, indicating that the atomic closed-shell calculation procedure accounts accurately for the transitions between the core levels in molecular iodine. The only obvious molecular effects in the $M_{4,5}N_{4,5}N_{4,5}$ spectra are the line broadening and the shift of the absolute energies due to extra-atomic relaxation phenomena. The broadening of the lines of molecular iodine is expected to arise from the excitation of a number of vibrational states in the intermediate and final ions.

B. $M_{4,5}N_{2,3}N_{4,5}$ spectra

From the $4p_{1/2}$ and $4p_{3/2}$ levels only one peak has been observed in the photoelectron spectra of xenon. This intensity anomaly has been studied in several papers.[20-22] The $N_2N_{4,5}N_{4,5}$ super Coster-Kronig transitions are energetically possible for

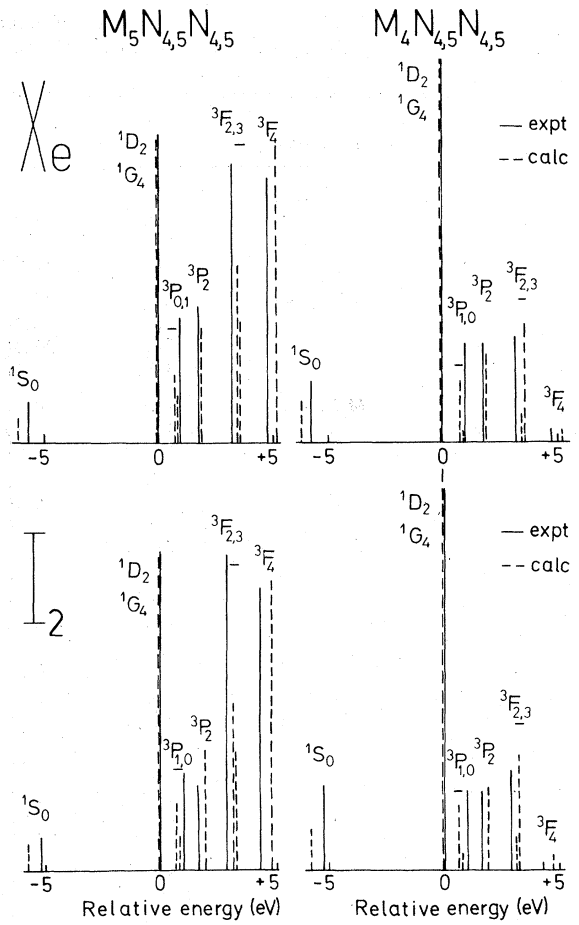

FIG. 10. Comparison between experimental and theoretical relative intensities and energies in the $M_{4,5}N_{4,5}N_{4,5}$ Auger spectra of Xe and I_2. The solid lines represent the experimental results (using 0.9-keV excitation) and the dashed lines the theoretical. The small horizontal marks indicate the total intensity of two theoretical intensities for lines that would not be resolved experimentally.

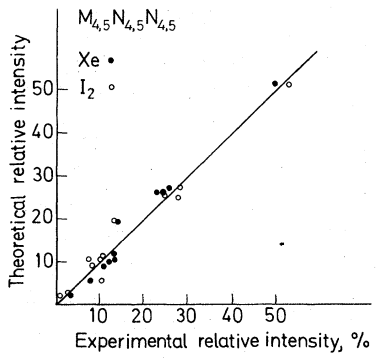

FIG. 11. Comparison between experimental and theoretical relative intensities in the $M_{4,5}N_{4,5}N_{4,5}$ Auger spectra of Xe and I_2.

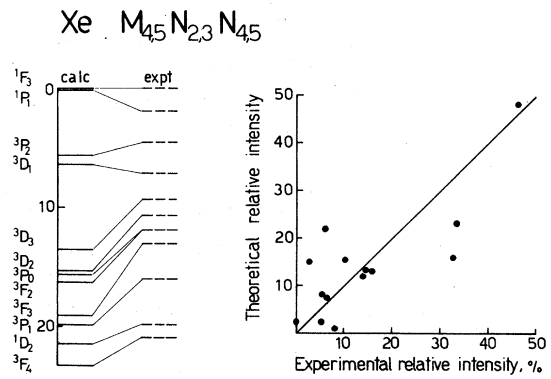

FIG. 12. Comparison between experimental and theoretical relative energies and intensities in the $M_{4,5}N_{2,3}N_{4,5}$ Auger spectra of Xe.

elements around xenon ($Z = 54$) and cause such strong lifetime broadening of the $4p_{1/2}$ level that no clear photoelectron peak can be seen from it. In addition there is strong configuration interaction with $4d^8 4f$ configurations causing the $4p_{1/2}$ intensity to be spread out over several levels. The energy of the state that corresponds to a $4p_{3/2}$ hole is 145.5 eV, below the threshold for the super Coster-Kronig process. Although this line is not broadened by the possibility of super Coster-Kronig transitions, its position is shifted by interaction with $4d^8 4f$ configurations by about 10 eV from the value obtained using relativistic Hartree-Fock calculations for the initial and final states. The final states populated in the $M_{4,5}N_{2,3}N_{4,5}$ Auger transitions involve the same $4p$ hole states; it is interesting to see whether similar effects are apparent in the Auger spectra.

We have decomposed the xenon Auger spectra into the components expected if an independent-particle model is valid. The results are shown in Fig. 6 and listed in Tables V and VI. We have also calculated the expected energies and intensities using the theoretical procedure outlined above; the results of these calculations are given in Tables V and VI, and in Fig. 12. In the left side of this drawing we show a comparison between the experimental and theoretical relative energies. In the right side we have plotted the theoretical relative intensity versus the experimental. The agreement here is not nearly so good as that shown in Figs. 10 and 11 for the $M_{4,5}N_{4,5}N_{4,5}$ spectra. The theory does, however, predict the major features of the spectrum. The shifts and line broadenings of the photoelectron spectrum are not apparent in the Auger spectrum. The inherent line width of the $M_{4,5}N_{2,3}N_{4,5}$ spectrum is only 0.6 eV greater than that for the $M_{4,5}N_{4,5}N_{4,5}$ spectrum. The experimental ratio of $M_4N_{2,3}N_{4,5}$ to $M_5N_{2,3}N_{4,5}$ intensities is 1:1 rather than the statistical value of 4:6. This deviation may at least partially arise from the problems of decomposing the $M_{4,5}N_{2,3}N_{4,5}$ spectrum, which has many lines of low intensity.

We have also calculated theoretical energies and intensities for the corresponding iodine Auger spectrum. The results are similar to those for xenon. The iodine experimental spectrum is, however, quite different from that of xenon and the agreement between experiment and independent-electron theory is quite bad for iodine. The energies of the final states in $M_{4,5}N_{2,3}N_{4,5}$ Auger transitions can be readily calculated from the $3d$ ionization energies and from the Auger energies. For xenon these energies range from 222 to 243 eV. These states are below the threshold for a super Coster-Kronig process that would convert the p hole to two d holes—the process that is responsible for the anomalous photoelectron spectra. We can estimate the threshold for production of a $4d^7$ configuration in the following way. The lowest $4d^8$ state in xenon is 151.5 eV (from the M_4 and M_5 binding energies and the $M_{4,5}N_{4,5}N_{4,5}$ Auger energies). If we ignore relaxation, then the energy required to remove one more d electron is 69 eV (the $4d$ ionization energy in neutral xenon) plus about 36 eV (twice the Coulomb interaction between pairs of $4d$ electrons in neutral xenon: twice because the newly formed hole interacts with both of the original holes). The minimum total energy of the $4d^7$ configuration is, accordingly, about 256 eV, significantly above the energy available in the $4p^5 4d^9$ manifold. Inclusion of relaxation effects will lower the estimate of the threshold; a more accurate estimate of the Coulomb interaction of the holes, allowing for shrinkage of the orbitals as the xenon is progressively ionized, will raise it. Since this energy is close to the energies of the $4p^5 4d^9$ states it seems likely that there will be interaction between $4p^5 4d^9$ and $4p^6 4d^7 4f$ configurations, similar to that found in the photoelectron spectra. Such configuration interaction could be responsible for the poorer agreement between experiment and theory for the $M_{4,5}N_{2,3}N_{4,5}$ Auger spectra.

For the Auger spectrum of iodine the situation is different. From the two peaks in the iodine $M_{4,5}N_{2,3}N_{4,5}$ Auger spectrum (Fig. 5) and the $4d_{3/2}$ ionization energy, the highest energy $4p^5 4d^9$ state in I_2 consistent with the observed Auger spectrum is 214 eV. (If the peak in the Auger spectrum at 424.6 eV arises from a $4d_{5/2}$ initial state, then the highest energy state is at only 205 eV.) Comparison of the xenon and iodine spectra suggests that there are missing transitions in the iodine spectrum corresponding to states of higher

energy. We estimate the threshold for the super Coster-Kronig process as before. The lowest $4d^8$ configuration in I_2 is at 128 eV, the $4d$ ionization energy in neutral I_2 is 58 eV, and the Coulomb interaction energy per pair is about 14 eV. The sum of these is 214 eV. The actual threshold is probably lower because of relaxation effects, which will be especially large in I_2 because of extra-atomic relaxation towards the triply charged hole. It is, therefore, likely that most of the iodine $4p^5 4d^9$ states are above the threshold for a super Coster-Kronig transition and that the peaks that would correspond to these final states are broadened beyond recognition. The only peaks remaining in the spectrum correspond to those final states that are below this threshold. The left-most peak may correspond to the $M_5N_{2,3}N_{4,5}$ ($^3P_0$, $^3F_{2,3}$) transitions and the right-most to a combination of $M_5N_{2,3}N_{4,5}$ ($^1D_2$, $^3F_4$) and $M_4N_{2,3}N_{4,5}$ ($^3D_{3,2}$, $^3P_0$, $^3F_{2,3}$). Since the spacing between the two groups is less than the $4d_{3/2}$-$4d_{5/2}$ spin-orbit splitting, we cannot assign these groups simply to the same final states originating in different $4d$ subshells.

C. $M_{4,5}N_{4,5}O_{1,2,3}$ spectra

The identification of the $M_{4,5}N_{4,5}O$ line groups is not straightforward because of overlapping and extra line groups. The $4d$ spin-orbit splitting in xenon is 12.6 eV and the binding energies for $5s$ electrons are about 11 eV higher than for $5p$ electrons. Thus the $M_4N_{4,5}O_1$ and $M_5N_{4,5}O_{2,3}$ line groups are expected to overlap. The calculated term splittings of components for $N_{4,5}O_1$ and $N_{4,5}O_{2,3}$ two-hole final states are rather small, 2–3 eV. These factors together with the rough group intensity and kinetic-energy considerations have led us to the conclusion that the strongest group consists of the partly overlapping $M_4N_{4,5}O_1$ and $M_5N_{4,5}O_{2,3}$ transitions. Thus in the spectrum of xenon the group around 597 eV is the $M_4N_{4,5}O_{2,3}$ group and around 573 eV the $M_5N_{4,5}O_1$ group. The broad lines 1′ and 2′ at 566 eV and at 577 eV (Fig. 8) are then assumed to be satellite line groups possibly associated with the $M_5N_{4,5}O_{2,3}$ and $M_4N_{4,5}O_{2,3}$ groups.

Valence electrons are directly involved in the iodine $M_{4,5}N_{4,5}O_{2,3}$ Auger transitions, because the $5p$ electrons are valence electrons in iodine. In spite of this fact the spectra of xenon and iodine are, however, very similar. The spectra of xenon have been decomposed into components and the relative line energies and intensities are given in Tables VII and VIII together with the calculated values. The agreement between theory and experiment is not so good as for the $M_{4,5}N_{4,5}N_{4,5}$ spectra. This lack of good agreement presumably arises because of the difficulty of resolving the overlapping spectra and possibly because configuration interaction may be more important for valence states than for core states.

D. Extra-atomic relaxation energies

The kinetic energy of Auger transitions (jkl) can be written in terms of one-electron binding energies, assuming that the independent-particle model is valid:

$$E_{jkl} = B_j - B_k - B_l - F(kl) + R(kl) \quad (1)$$

where B_j, B_k, and B_l are the binding energies of j, k, and l levels, $R(kl)$ accounts for the total (static) relaxation energy of the two-hole final state, and $F(kl)$ gives the interaction energy of the two final-state holes. This model can be used for the $M_{4,5}N_{4,5}N_{4,5}$ transitions, where the initial and final states are accurately described by an independent-electron model, but may not be valid for $M_{4,5}N_{2,3}N_{4,5}$ transitions, where the final states are not one-electron states but apparently multielectron states. When the binding energies and the kinetic energy of the Auger line are measured and the interaction energy $F(kl)$ can be calculated using the standard multiplet theory, the relaxation energy term $R(kl)$ in Eq. (1) can be estimated. Thus using the experimental binding energies from Ref. 19 for Xe and our measured values for I_2 and the two-electron integral values tabulated by Mann[15] we obtain for $M_{4,5}N_{4,5}N_{4,5}$ spectra from Eq. (1) 11.6 and 8.9 eV for the total relaxation energies $R(kl)$ of I_2 and Xe, respectively. The total relaxation energies can be formally divided into atomic and extra-atomic parts. In the case of xenon we have only atomic relaxation energy but for the iodine molecule also the extra-atomic contribution. The change in the atomic relaxation energy for the adjacent elements iodine and xenon is rather small. According to the calculations of Wendin and Ohno[20] the atomic relaxation contribution is 0.28 eV lower for iodine than xenon. As a first approximation in the Auger process the effect of atomic relaxation energy should be taken twice giving a correction of 0.56 eV. Thus the difference in the calculated energies using Eq. (1) for these two elements is mainly caused by extra-atomic relaxation energy of molecular I_2. The possible systematic errors in calculating the hole-hole interaction energy $F(4d, 4d)$ will be cancelled to large extent in the calculation of the difference of the total relaxation energies between xenon and iodine. From these values we conclude that the extra-atomic relaxation energy term of the $M_{4,5}N_{4,5}N_{4,5}$ Auger transition in I_2 is

3.3 eV. It should be noted that this is not directly the observed energy shift between molecular and atomic Auger spectra because extra-atomic relaxation is also involved in the experimental one-electron binding energies.

E. Photoelectron spectra

In iodine the energy of the $^1G_4$ component of the $4d^2$ two-hole configuration is 132.0 eV.[24] Thus the binding energy of the $4p_{3/2}$ level 129.9 eV is only 2.1 eV lower than the energy of the $4d^2$ ($^1G_4$) state but is slightly higher than the energies of $4d^2$ (^3F) components. Hence the binding energy of $4p_{3/2}$ level is just on the energy limit of $N_3N_{4,5}N_{4,5}$ super Coster-Kronig transitions allowing energetically transitions to the $4d^2$ (^3F) final states. This explains the odd shape of the $4p_{3/2}$ photoline. In the case of the xenon the energies of the $4d^2$ final-state components are above the observed $4p_{3/2}$ ionization energy and the $4p_{3/2}$ photoline looks more ordinary. For both elements the $4p_{1/2}$ binding energies are clearly above the energies of $4d^2$ two-hole states and because of the very high transition probabilities of super Coster-Kronig transitions $4p_{1/2}$ levels are strongly lifetime broadened and smeared out from the photoelectron spectra.

V. SUMMARY

For the $M_{4,5}N_{4,5}N_{4,5}$ Auger spectra of both atomic xenon and molecular iodine the relative intensities and relative energies are given accurately by an independent-electron model. There is no evidence for many-body effects in these spectra. The molecular spectra differ from the atomic spectra in that the inherent width of the peaks is greater (0.92 eV for I_2 compared with 0.64 eV for Xe) and the absolute values of the iodine Auger energies are shifted from those expected for free atoms because of extra-atomic relaxation. The line broadening presumably arises because a wide variety of vibrational states are populated in either the initial or final states of the Auger process. The extra-atomic relaxation is determined to be about 3.3 eV in iodine.

The $M_{4,5}N_{2,3}N_{4,5}$ spectrum for I_2 is quite different from that for Xe, in contrast to the $M_{4,5}N_{4,5}N_{4,5}$ spectra, which are quite similar for the two substances. The independent-electron calculations for xenon predict only the overall features of the spectrum and do not agree well with experiment. Similar calculations for iodine are in strong disagreement with the experimental results. The failure of the independent-particle model is associated with the well-known many-electron character of the $4p$ hole state. Consideration of the energies of the various two- and three-hole states shows why these effects are stronger in the spectrum of iodine than in that of xenon.

Even though the $M_{4,5}N_{4,5}O$ Auger spectra involve the molecular orbitals of iodine, there is still a good resemblance between the xenon and iodine spectra. Agreement between the independent-electron calculations and the experimental results for xenon is not so good as for the $M_{4,5}N_{4,5}N_{4,5}$ spectra.

ACKNOWLEDGMENTS

This work was supported in part by the NSF. Acknowledgment is made to the Donors of The Petroleum Research Fund, administered by the American Chemical Society, for partial support of this research.

[1]S. Hagmann, G. Hermann, and W. Mehlhorn, Z. Phys. 266, 189 (1974).
[2]L. O. Werme, T. Bergmark, and K. Siegbahn, Phys. Scr. 6, 141 (1972).
[3]C. J. Powell, Rev. Mod. Phys. 48, 33 (1976).
[4]P. H. Citrin, R. W. Shaw, Jr., and T. D. Thomas, in *Electron Spectroscopy*, edited by D. A. Shirley (North-Holland, Amsterdam, 1972), p. 105.
[5]T. D. Thomas and R. W. Shaw, Jr., J. Electron Spectrosc. 5, 1081 (1974).
[6]C. E. Moore, Natl. Bur. Stand: (U.S.), Circ. No. 467, Vol. 1 (1949).
[7]G. Johansson, J. Hedman, A. Berndtsson, M. Klasson, and R. Nilsson, J. Electron Spectrosc. 2, 295 (1973).
[8]Because of vibrational broadening in the molecular I_2, the line shape for this substance may, in fact, not be Lorentzian.
[9]H. Aksela, S. Aksela, J. S. Jen, and T. D. Thomas, Phys. Rev. A 15, 985 (1977).
[10]H. Aksela and S. Aksela, J. Phys. B 7, 1262 (1974).
[11]S. Aksela, J. Väyrynen, and H. Aksela, Phys. Rev. Lett. 33, 999 (1974).
[12]H. Aksela (unpublished).
[13]J. C. Slater, *Quantum Theory of Atomic Structure* (McGraw-Hill, New York, 1960).
[14]E. U. Condon and G. H. Shortley, *Theory of Atomic Spectra* (Cambridge University, Cambridge, England, 1970).
[15]J. B. Mann, Los Alamos Scientific Laboratory Report LA-3690, 1967 (unpublished).
[16]K-H Huang, M. Aoyagi, M. H. Chen, B. Crasemann, and H. Mark, At. Data Nucl. Data Tables 18, 243 (1976).
[17]B. W. Shore and D. H. Menzel, *Principles of Atomic Spectra* (Wiley, New York, 1968).
[18]E. J. McGuire, Sandia Research Laboratories Re-

search Report No. SC-RR 71 0835 (1972) (unpublished).
[19]U. Gelius, J. Electron Spectrosc. Relat. Phenom. 5, 985 (1974).
[20]G. Wendin and M. Ohno, Phys. Scr. 14, 148 (1976).
[21]K. Siegbahn, C. Nordling, G. Johansson, J. Hedman, P. F. Hedén, K. Hamrin, U. Gelius, T. Bergmark, L. O. Werme, R. Manne, and Y. Baer, *ESCA Applied to Free Molecules* (North-Holland, Amsterdam, 1969).
[22]S. Svensson, N. Mårtensson, E. Basilier, P. Å. Malmquist, U. Gelius, and K. Siegbahn, Phys. Scr. 14, 141 (1976).
[23]E. J. McGuire, Phys. Rev. A 5, 1052 (1972).
[24]Calculated from the difference between the ionization energy of the M_4 level, 638.7 eV, and the kinetic energy of the $M_4N_{4,5}N_{4,5}$ ($^1G_4$) Auger line, 506.7 eV.